On the stability of electrochemical CO_2 reduction reaction to formate at indium electrodes at biocompatible conditions

Paniz Izadi, Aykut Kas, Philip Haus, Falk Harnisch[*]

Department of Environmental Microbiology, Helmholtz-Centre for Environmental Research - UFZ, Leipzig, Germany

A B S T R A C T

In a circular economy, carbon dioxide (CO_2) has to serve as feedstock that can be utilized by electrochemical CO_2 reduction reaction (eCO_2RR). Using eCO_2RR to C_1-compounds such as formate ($HCOO^-$) allows producing feed for microbial syntheses that generates value-added compounds. However, eCO_2RR at biocompatible conditions is currently limited to short-term operation facing a gradual performance deterioration. Here, we evaluate the possible parameters affecting the stability of performance in terms of formate production rate (r_{HCOO^-}) and coulombic efficiency (*CE*) of eCO_2RR at indium during 72 h batch mode operation. Formate accumulated over time affected catholyte conductivity, but statistical analysis showed this did not have an immediate influence on the performance. However, both are key factors altering the actual cathode potential over time that in turn is leading to changes in r_{HCOO^-} (maximum deviation of $\pm$ 0.03 mmol h^{-1} cm^{-2} at the stable performance at each condition) and *CE* (maximum deviation $\pm$ 40% at stable performance at each condition). These effects were more significant after reaching certain formate concentration and catholyte conductivity (*ca.* 70 mM and 21 mS cm^{-1}, respectively). These results highlight the potential obstacles needed to be considered and tackled in order to achieve stable r_{HCOO^-} and *CE* over a long-term eCO_2RR operation. This study discusses how to overcome these obstacles from different operational perspectives.

1. Introduction

Due to the growing population and mankind's lifestyle on earth the atmospheric levels of carbon dioxide (CO_2) are rising. It is increasing societal consensus that there is an urgent need to decrease the CO_2 emission and develop technologies utilising CO_2 as a carbon feedstock. Utilisation of CO_2 and its conversion to chemicals and fuels pave the way towards circular economy [1]. Offering the possibility to be operated at mild reaction conditions (e. g. ambient temperature and atmospheric pressure), the electrochemical CO_2 reduction reaction (eCO_2RR) is highly promising for converting CO_2 to chemical products, in particular C_1-compounds such as formate [2]. Due to the large amount of energy required for dissociation of the C=O bond (795 kJ mol^{-1}) that is needed for activation of CO_2 molecules, electrocatalysts are required for the eCO_2RR [3]. By far, numerous materials such as tin (Sn), tin oxide (SnO$_2$) and especially copper (Cu) have been proposed as electrocatalysts for eCO_2RR [4]. Using Cu for eCO_2RR for instance, a variety of products ranging from formate ($HCOO^-$) and carbon monoxide (CO) to the compounds needing a C-C-bond formation such as ethylene (C_2H_4)

were detected [5]. Methane (CH_4) was reported as a product of eCO_2RR using binary colloidal Cu and silver (Ag) nanoparticles [6]. For process development and engineering, the selective production of one compound is often required rather than a high diversity of products. Indium (In) is an electrocatalyst with high selectivity for formate with a notable coulombic efficiency (*CE*) of even higher than 90%, being used for eCO_2RR on different supports (e.g. carbon black) [7]. For instance, In$_2$O$_3$ nanoparticles were synthesized on carbon black for eCO_2RR [8]. The authors reported the *CE* of 87% for formate production at the cathode potential of -0.9 V vs. RHE in 0.5 M KHCO$_3$ electrolyte solution [8]. Previously, we investigated the eCO_2RR to formate using electrodeposited In on carbon electrodes as electrocatalyst at biocompatible conditions, especially neutral pH as well as ambient temperature and pressure, in a lab scale (50 mL) [9] as well as scaled-up (1 L) [10] electrobioreactors. Over 1 h of eCO_2RR at the applied potential ($E_{applied}$) of -2.2 V vs. Ag/AgCl sat. KCl, respective formate production rates (r_{HCOO^-}) of 0.061 and 0.038 mmol h^{-1} cm^{-2}, and *CE* of 94% and 74% were achieved in the lab scale and scaled-up reactors [9,10].

Microbial based technologies offer another platform for conversion

of CO_2 to value-added chemicals. Syngas fermentation is among the most prominent platforms, in which microorganisms either reduce CO_2 as a carbon source using hydrogen (H_2) as an energy source or exploit CO [11]. Generally, more diverse and especially more energy rich products can be achieved from CO_2 through microbial pathways than by eCO_2RR (e.g. typically C_2- to C_8-compounds [12,13] compared to C_1- to C_2-compounds [2], respectively). However, the rate of microbial processes is usually lower than of eCO_2RR. For instance, a maximum microbial production rate of 0.093 mol L^{-1} d^{-1} caproate (hexanoate) under optimal conditions through addition of desired substrates in open-culture biotechnological reactors is reported [14]. In addition, providing the constant energy source for microbial CO_2 reduction is still a challenge due to the low solubility of H_2 in aqueous solutions (1.6 mg L^{-1}, 293 K and 1 atm), leading to its low and often limited availability for microbial production [15,16]. Considering the advantages of high rates and selectivity of eCO_2RR, linking it to microbial production seems highly promising, as more valuable products than C_1-compounds but with higher production rate can be achieved [17]. As formate can serve as both carbon and energy sources for microbial metabolisms, it can be considered as a suitable substrate in order to produce value-added compounds [18]. The first proof was reported by Li et al [19]. In their study, formate produced from CO_2 at In electrodes was used by genetically engineered *Ralstonia eutropha* (currently known as *Cupriavidus necator*) for production of higher alcohols. Production of the polymer polyhydroxyrate (PHB) by the microorganism of *Cupriavidus necator* using formate gained through eCO_2RR is another example for production of valuable compounds from CO_2 through integrating electrochemical and microbial syntheses [20]. In addition to pure cultures, microbial mixed cultures were also used and acetate and methane were microbially produced from CO_2 using formate from the eCO_2RR at copper electrodes [21].

For future process engineering and steering, deciphering the impact of environmental as well as operational parameters on the eCO_2RR at biocompatible conditions is required. Thereby, one main concern is performance stability over time and its consistency across studies. For In cathodes, the optimal CE and r_{HCOO^-} achieved during the first hour seemed not to remain stable over time [22]. As operation over days up to weeks or even months is required, performance decline limits the applicability of eCO_2RR. A few reasons are considered to cause the performance decline. One is related to H_2 evolution reaction (HER) [23] that is not only competing with eCO_2RR and thus lowering CE and r_{HCOO^-}, but may also lead to the leaching of electrocatalysts, e.g. by spalling off [24]. In addition, various operating conditions can affect the eCO_2RR as well as HER and other side-reactions over the long-term operation. One of these is the electrolytic conductivity of the solution (κ_S). Due to its correlation with the internal resistance including the $i \times R$-drop, the activity and selectivity of eCO_2RR may vary with κ_S and at different electrolyte composition [25]. However, it is still unknown to what extend these as well as other operational parameters do affect the performance of eCO_2RR over a longer-term operation than few hours.

In our previous study on eCO_2RR to formate using In deposited graphite rod as a cathode, we showed that the highest CE was achieved at the $E_{applied}$ of -2.2 V vs. Ag/AgCl sat. KCl with 90% [9]. As these results were derived from 1 h operation, here we investigated the longer-term operation of 72 h using the identical setup. We deciphered the effects of different cathode potentials (ranging from -2.2 to -1.6 V vs. Ag/AgCl sat. KCl), presence of already accumulated formate, and catholyte conductivity on long-term operation of eCO_2RR to formate as well as electrode corrosion.

2. Experimental

2.1. General statements

All potentials in this study are reported vs. Ag/AgCl in saturated KCl (0.197 V vs. standard hydrogen electrode (SHE)) if not stated otherwise.

All chemicals were of at least analytical grade. All solutions were prepared with de-ionized water (Merck Millipore, USA). All experiments were performed in triplicate (except the conductivity experiment, which was performed in quadruplicate), and the results are reported as average with standard deviation. Time point t=0 mentioned throughout the manuscript refers to the data recorded when starting the eCO_2RR experiments.

2.2. Experimental setup

The experimental setup was identical to the previously used one [9]. In brief, a two-chamber electrochemical cell with a 300 mL glass reactor serving as a working electrode (WE, cathode) compartment was used (Fig. 1). The reactor was equipped with the 3D printed polylactic acid (PLA) lid. The lid contained several ports that allowed placing the electrodes fixed throughout the experiments as well as sampling [9,22]. The counter electrode (CE, anode) was inserted in a glass custom-made tube which was interfaced to the reactor using a cation exchange membrane (CEM, fumasep FKE, FuMA-Tech GmbH, Germany). The cathode was a graphite rod of high purity (99.997 %, Ø 0.635 × 6 cm, C-00-RD-000121, Goodfellow, UK) with a net geometric surface area (inserted in the solution) of 2.5 cm^2 connected to the rotating electrode holder (CTV 101T, Tacussel, France). CEs were platinized titanium (Ti) plates (0.05 × 1 × 7 cm, platinode, Umicore Galvanotechnik GmbH, Germany) and reference electrodes (RE) were Ag/AgCl in saturated KCl (SE 11, +0.197V vs. SHE, Xylem Analytics Germany Sales GmbH & Co. KG Sensortechnik Meinsberg, Germany), respectively. To perform the experiments under potentiostatic mode, a potentiostat (SP-50, BioLogic Science Instruments, France) was used, while a DC-power supply (Keithley 2230-30-1, Keithley Instruments, USA) was used for galvanostatic operation. Although $E_{applied}$ at the cathode electrode was controlled by the potentiostat, the actual electrode potential (E_{WE}) was still measured against RE. For measuring the internal resistance, electrochemical impedance spectroscopy (EIS) was performed under open circuit potential (OCP) using frequencies between 100 kHz and 0.1 Hz with an amplitude of 20 mV.

Before and during the eCO_2RR a constant CO_2 flow of 1.2 vvm was provided using a rotameter (Influx Measurement, United Kingdom) to the cathode compartment passed through a wash bottle containing water to humidify the gas and prevent evaporation. Both catholyte and anolyte were 50 mL, 0.05 M $NaHCO_3$ (pH 6.5). The catholyte was constantly stirred using a magnetic stir bar at 1,000 rpm. Prior to use, all glassware and reactor components were UV sterilized in biosafety cabinets (Maxisafe-2030i, Thermo Scientific, Germany). Anolyte was continuously refreshed with a peristaltic pump (ISMATEC Reglo Analog MS-4/8, Cole-Parmer GmbH, Germany) to the anode compartment with flow rate of 1.2 mL min^{-1}. All eCO_2RR experiments were conducted at 30°C in an incubator hood (TH 30, Edmund Bühler GmbH - 72411 Bodelshausen Germany).

2.3. Pre-treatment and In deposition on the WE

Pre-treatment and In deposition was performed as described previously according to the optimal conditions [22] that were later slightly modified [9]. After mechanical and electrochemical pre-treatment of the graphite electrode, In was electrochemically deposited. During the electrodeposition step, electrode holder rotated at 10 rpm to assure a homogenous coverage of the graphite rod with In. Electrodeposition was performed at -0.9 V with the defined charge of 1.7 C. The solution for electrodeposition step was 50 mL of 0.1 M $InCl_3$ (anhydrous, 99.999%, Chempur, Germany) in 1 M acetate buffer (pH 4.5) in a single chamber reactor and was sparged with N_2 at 1.6 vvm flow rate adjusted with a rotameter (Influx Measurement, UK). After electrodeposition, 2.5 cm^2 net surface area of the electrode was covered with maximum 2,200 theoretical atomic layers of In [9]. The pre-treatment and electrodeposition steps were carried out independently before each single eCO_2RR
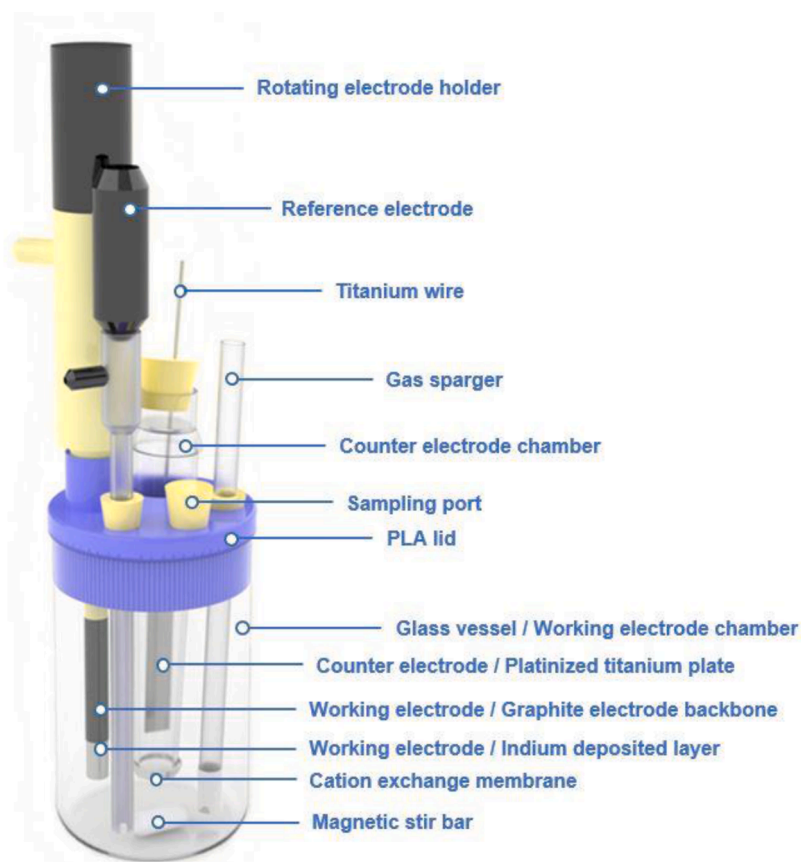
Fig. 1. Schematic of the reactor used in electrochemical CO_2 reduction experiments in this study (details see text).

experiment. Before using the In-coated graphite electrodes for the eCO_2RR experiments, they were rinsed with deionized water.

2.4. Chemical analyses

Throughout the eCO_2RR experiments, 400 μL catholyte samples were collected through a sampling port regularly (every 2 hours during the daytime). Samples were analyzed using a pH electrode (InLab Micro Pro, Mettler Toledo, Switzerland) and a conductivity probe (InLab 731-ISM, Mettler Toledo, Switzerland) connected to the pH/conductivity benchtop meter (S470, Mettler Toledo, Switzerland). To detect the products, liquid phase analysis was conducted with an HPLC (Shimadzu Scientific Instruments, USA) equipped with a refractive index detector (RID) (RID-20A, Shimadzu Scientific Instruments, Japan) Hi-Plex H column (300 mm × 7.7 mm ID, 8 μm pore size, Agilent Technologies, Germany) with a pre-column (Carbo-H 4 mm × 3 mm ID, Security Guard, Phenomenex). Isocratic elution was performed with 0.005 M H_2SO_4 at 0.5 mL min^{-1} at 50°C for 30 min^{-1}. Formate was the only product from eCO_2RR detected in the catholyte. Calibration of formate (1.14 mM to 44.4 mM, five-point calibration with triplicate standards for each point, R^2= 0.99) was carried out with external standards.

To measure In leached in the catholyte, 5 mL sample was collected from the solution every 24 hours, and was replaced by the 5 mL fresh solution. In case of possible change in the formate concentration (c_{HCOO-}) after replacing the medium, it was measured after each sampling for In measurement. The concentration of In was measured using polarography (797 VA Computrace, Metrohm, Switzerland) equipped with platinum wire as CE and a Ag/AgCl in saturated KCl as RE by differential pulse (DP) mode at a hanging mercury drop electrode (HMDE) [26]. Calibration was conducted with external In standards (0.906 nM to 0.906 mM, three-point calibration, R^2= 0.99) prepared in triple distilled water. To assure the credibility of the data from

polarography, samples were randomly selected and measured additionally using ELEMENT$_{TM}$XR sector field ICP-MS (Thermo Fisher Scientific, Germany) and compared with the results from the polarography (Table S1). Due to the resemblance of the data, all the samples were measured using polarography.

2.5. Data processing and statistical analyses

CE was calculated for the eCO_2RR to formate from the total amount of charge (Q_{total}) and theoretical amount of charge (Q_{HCOO-}) required for the amount of formate (n_{HCOO-}) measured with HPLC:

$$CE\ (\%) = \frac{Q_{HCOO^-}}{Q_{total}} = \frac{n_{HCOO^-} \times z \times F}{\int_{t=0}^{t} Idt} \times 100 \qquad (1)$$

with z=2 being the number of electrons transferred per CO_2 molecule and F being the Faraday's constant (96,485 C mol^{-1} C). All the CE values reported within the manuscript were calculated at a certain time interval between the given and last sampling points.

The rate of formate production r_{HCOO-} was calculated based on the amount of formate produced (n_{HCOO-}) between sampling points (dt) and net surface area of the In-coated graphite electrode (A= 2.5 cm^2):

$$r_{HCOO^-}\left(\frac{mmol}{cm^2\ h}\right) = \frac{n_{HCOO^-}}{A \times dt} \qquad (2)$$

The formal potentials for eCO_2RR to formate ($E_{CO_2/HCOO-}^{0\#}$) and HER ($E_{2H+/H_2}^{0\#}$) were calculated (Eqs. (4) and (7)) using the standard electrode potentials for these reactions ($E_{CO_2/HCOO-}^{0}$=-0.22V vs. SHE and E_{2H+/H_2}^{0}= 0 V vs. SHE, respectively calculated using the Gibbs free energy of individual species at pH=0 extracted from [27]), molar gas constant R=8.314 J mol^{-1} K^{-1} and temperature T=303.15 K. Equilibrium

constant of the reaction calculated using c_{HCOO^-} measured by HPLC, pH of the samples and saturated concentration of CO_2 and H_2 gasses (c_{CO2} and c_{H2}, respectively) under the experimental conditions (Table S9). Overpotentials ($\eta_{CO_2/HCOO^-}$ and η_{2H+/H_2}) were calculated (Eqs. (5) and (8)) from the actual E_{WE} at the sampling times measured with either a digital multimeter (RS PRO RS-14, RS Components GmbH, Germany) or from the continuous data recorded by potentiostat/galvanostat and the electrode potentials ($E_{CO_2/HCOO^-}^{0\#}$ and $E_{2H+/H_2}^{0\#}$) calculated through experimental conditions and concentrations of reactants.

$$CO_2 + 2e^- + H^+ \rightarrow HCOO^- \tag{3}$$

$$E_{CO_2/HCOO^-}^{0\#} = E_{CO_2/HCOO^-}^0 - \frac{RT}{zF}\ln Q = E_{CO_2/HCOO^-}^0 - \frac{RT}{zF}\ln\left(\frac{c_{HCOO^-}}{c_{H^+} \times c_{CO_2}}\right) \tag{4}$$

$$\eta_{CO_2/HCOO^-} = E_{WE} - E_{CO_2/HCOO^-}^{0\#} \tag{5}$$

$$2H^+ + 2e^- \rightarrow H_2 \tag{6}$$
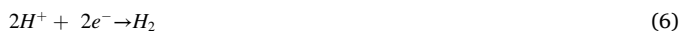
$$E_{2H+/H_2}^{0\#} = E_{2H+/H_2}^0 - \frac{RT}{zF}\ln Q = E_{2H+/H_2}^0 - \frac{RT}{zF}\ln\left(\frac{c_{H_2}}{(c_{H^+})^2}\right) \tag{7}$$

$$\eta_{2H+/H_2} = E_{WE} - E_{2H+/H_2}^{0\#} \tag{8}$$

In order to evaluate the effect of different parameters (i.e. independent variables) on the performance of the eCO$_2$RR, statistical analyses were performed. These selected independent variables were E_{WE}, c_{HCOO^-} and κ_S and their effects on the system performance were studied (Table S2). To monitor the effect of cathode potential, the results of the triplicate experiments at 4 different $E_{applied}$ (-1.6, -1.8, -2.0 and -2.2 V) were considered. The effect of c_{HCOO^-} was monitored using the results from the separate quadruplicate experiments, in which 70 mM formate was manually added to the catholyte at t=0. To assess the effect of κ_S on the eCO$_2$RR performance in separate triplicate experiments, 17 g L^{-1} sodium sulphate (Na$_2$SO$_4$) was added to the catholyte at t=0, leading a κ_S of 23.0 ± 0.1 mS cm^{-1} being identical to the catholyte κ_S achieved after 24 h under $E_{applied}$ of -2.2 V. Due to the difference observed between the values of $E_{applied}$ and E_{WE} over time (see results), E_{WE} was used in all the statistical analyses.

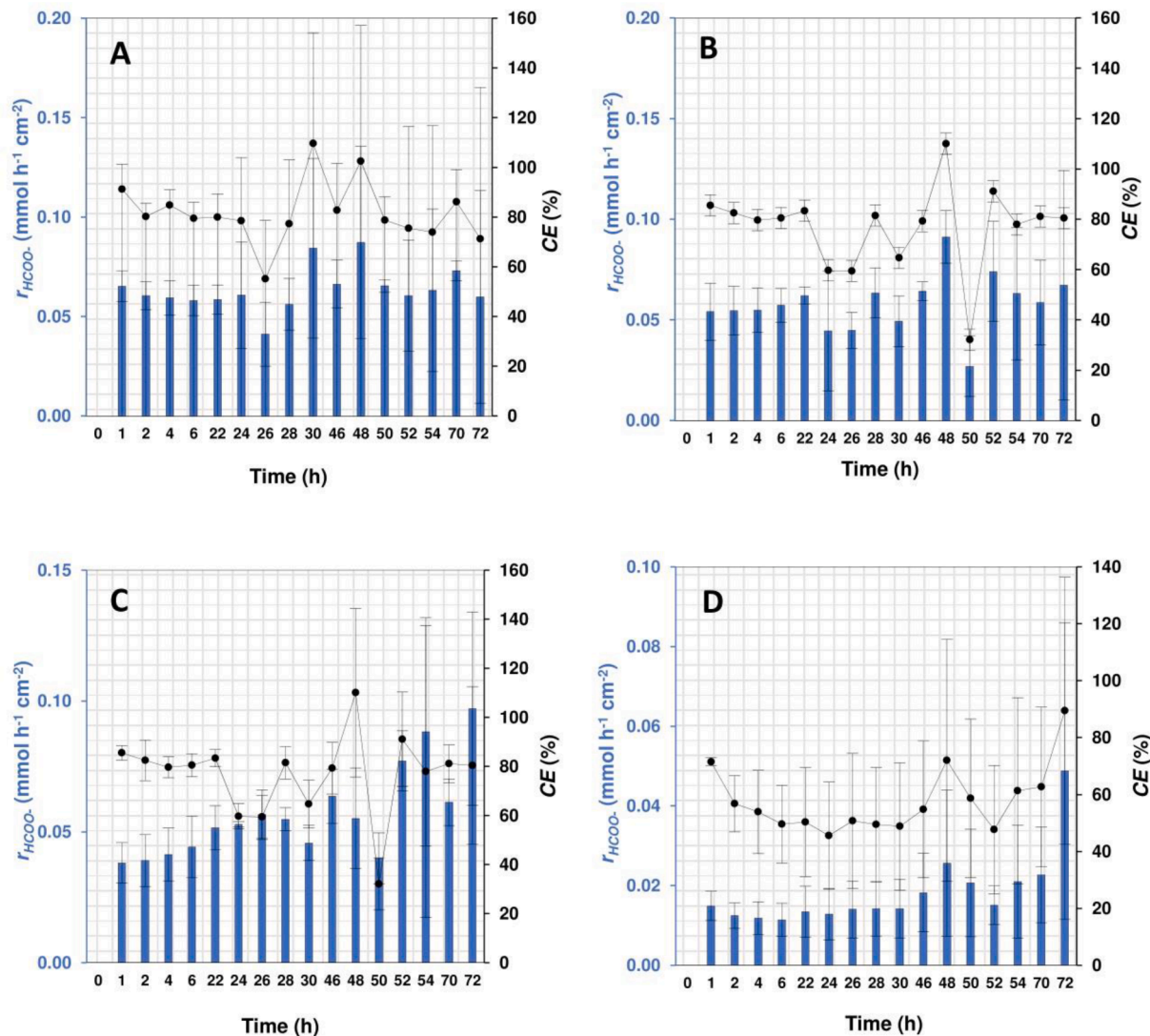All the statistical analyses were performed using R [28]. When the

Fig. 2. Formate production rate (r_{HCOO^-}) and coulombic efficiency (CE) during electrochemical CO$_2$ reduction to formate at 4 different applied potentials ($E_{applied}$) of A) -2.2 V, B) -2.0 V, C) -1.8 V, and D) -1.6 V. All experiments were conducted for 72 h, in 0.05 M NaHCO$_3$ (pH 6.5) as electrolyte solutions and in triplicate (n=3). Reported values are mean values and the error bars represent the confidence interval ($\alpha = 0.05$).

multiple dependent variables were considered, multivariate analysis of variance (MANOVA) test was used. MANOVA tests (and analysis of variance (ANOVA) tests, when required) were performed using "stats" package in R [29]. To visualize the data, the box-plots were plotted using "ggplot2" package in R [30].

3. Results and Discussions

3.1. 72 h-operation of eCO$_2$RR to formate at different potentials

For 1 h eCO$_2$RR, an $E_{applied}$ of -2.2 V was shown as an optimum for production of formate with more than 90% of CE at In electrodes [9]. Therefore, it was selected for a 72 h-operation. Formate production began immediately and $r_{HCOO-} = 0.061 \pm 0.002$ mmol cm^{-2} h^{-1} and CE = 82.3 ± 4.8 % were almost stable over the first few hours up to 24 h (Fig. 2), in line with our previous study at the $E_{applied}$ of -2.2 V [9]. Although similar r_{HCOO-} and CE were calculated for operation from 24 h to 72 h, strong fluctuations were observed. This was assumed to be related to HER competing with eCO$_2$RR, although H$_2$ in the headspace was not measured during the experiment due the constant CO$_2$ flushing. HER could contribute to 1) the gradual increase in pH of the catholyte over time (from *ca.* 6.4 at *t*=0 to 7.5 at *t*=72 h) due to decrease of proton concentration (Eq. 6) and lead to 2) increase in the indium leaching in the solution (Table S3). The increase in the leaching rate (from *ca.* 37 at 24 h to 780 ng mL^{-1} day^{-1} at 72 h, or considering the cathode surface from *ca.* 733 at 24 h to 15,606 ng cm^{-2} day^{-1} at 72 h) could be related to the increasing generation of H$_2$ bubbles at the surface of the electrode, leading to spalling off of In particles. The reason for occasional increase in CE to more than 100% was not clear. However, a similar trend was also observed in separate experiments with the $E_{applied}$ of -2.0 and -1.8 V, in which a CE of *ca.* 120% was measured after 48 h of operation (Fig. 2). Diffusion of formate through the cation exchange membrane (CEM) due to the concentration gradient can be excluded, as no formate was detected in the anode compartment of all reactors.

On the contrary, r_{HCOO-} and CE (in average 0.018 mmol h^{-1} cm^{-2} and 60%, respectively) calculated at the $E_{applied}$ of -1.6 V was almost stable over the 72 h-operation. Interestingly, sudden strong fluctuations in r_{HCOO-} and CE began after 24, 30 and 46 h at the $E_{applied}$ of -2.2, -2.0 and -1.8 V, respectively. These time points at different potentials had two facts in common: 1) reaching a similar c_{HCOO-} accumulated in the catholyte (*ca.* 70 mM), and 2) reaching a similar catholyte conductivity (κ_S of *ca.* 21 mS cm^{-1} from initially 4.5 mS cm^{-1}). We speculated that these two factors as well as change in pH may have caused the occasional inconsistencies and thus studied them further.

3.2. Set and actual cathode potential and statistical analysis of pH, κ_S and c_{HCOO-}

During eCO$_2$RR using a conventional potentiostat we noticed that the E_{WE} monitored against RE were different from $E_{applied}$ (-2.2, -2.0 and -1.8 V, Tables S4-7). At the $E_{applied}$ of -2.2 V, the E_{WE} began to change few hours after starting the experiment and reached to almost -1.7 V. Similar potential change was recorded at $E_{applied}$ of -2.0 and -1.8 V, in which the E_{WE} increased and reached to -1.7 V, this was not the case at $E_{applied}$ of -1.6 V. In order to check if this was related to the operational mode, an almost identical experiment was performed but using galvanostatic operation. Here, the current of -15 mA was fixed using a DC power supply, which corresponded to the current during potentiostatic operation with $E_{applied}$ of -2.2 V. However, similar to the potentiostatic operation the E_{WE} changed to around -1.7 V over time (Table S8).

Due to the difference between the $E_{applied}$ and E_{WE}, the latter was used as an independent variable for statistical analysis, thus the effect of E_{WE} on c_{HCOO-}, CE, r_{HCOO-}, and pH was studied. MANOVA test (p-value= 2.2 × 10^{-16}) showed that there was at least one group different from others. The summary of the MANOVA test revealed the significant relationship between the E_{WE} and c_{HCOO-} (p-value = 1.741 × 10^{-2}), CE (p-value = 2.487 × 10^{-2}), r_{HCOO-} (p-value = 1.068 × 10^{-4}), and pH of the catholyte (p-value = 2.397 × 10^{-8}) which can be also observed in the boxplots by differences in medians (Fig. 3). The effect of E_{WE} on eCO$_2$RR to formate is also in agreement with previous studies, although in these studies the E_{WE} was not measured but being assumed identical to $E_{applied}$ and considered stable over time [9]. The two parameters impacting the E_{WE} and hence the eCO$_2$RR performance were further evaluated.

3.3. The effect of c_{HCOO-} in the catholyte on the eCO$_2$RR

One of the two variables showing a probable effect on the fluctuation of r_{HCOO-} and CE was reaching a c_{HCOO-} of *ca.* 70 mM. Therefore, eCO$_2$RR at the $E_{applied}$ of -2.2 V was performed with this formate concentration being already present at the beginning of the experiment. Visually, the now obtained r_{HCOO-} and CE seemed similar to the values after 24 h when no formate was provided initially (Fig. 2A) including observed fluctuations (Fig. 4A). However, MANOVA and further ANOVA tests showed no significant correlation between the accumulated formate and r_{HCOO-} (p-value = 0.6618) or CE (p-value = 0.8494), which can also be seen in the box-plots (Fig. 4B). On the other hand, c_{HCOO-} seemed to significantly affect the E_{WE} (p-value= 2.2 × 10^{-16}) and pH (p-value= 2.2 × 10^{-16}). Therefore, we assume that a gradual increase in the c_{HCOO-} leads to the change in E_{WE} being different from $E_{applied}$, which influences r_{HCOO-} and CE and this leads to the occasionally observed fluctuations.

It is worth mentioning that at the initial eCO$_2$RR at $E_{applied}$ of -2.2 V without formate addition, the κ_S was *ca.* 5 mS cm^{-1}, whereas addition of 70 mM formate to the catholyte changed the κ_S value to *ca.* 9 mS cm^{-1} (Table S5). This showed that the κ_S of 21 mS cm^{-1} after 24 h when 70 mM formate was accumulated by eCO$_2$RR (Fig. 2A) was mostly related to charge balancing ion transfer through the membrane [31] and not to formate accumulation.

3.4. The effect of κ_S of the catholyte on the eCO$_2$RR

One of the important parameters in eCO$_2$RR is κ_S. A conductive solution is required to facilitate charge balancing ion transfer at low internal resistance. Internal resistance is not only important for the entire electrochemical cell and hence for the electric power per produced product, but also for the $i \times R$-drop between RE and WE [32]. In the eCO$_2$RR at the $E_{applied}$ of -2.2 V, κ_S was almost 5 mS cm^{-1} at *t*=0, however it increased one order of magnitude after 72 h, reaching *ca.* 48 mS cm^{-1}. Similar increase in the κ_S was also observed in the eCO$_2$RR at $E_{applied}$ of -2.0 and -1.8 V. As mentioned above, the occasional fluctuation in the r_{HCOO-} and CE appeared to start after reaching κ_S of *ca.* 21 mS cm^{-1}. Therefore, in separate experiments 17 g L^{-1} Na$_2$SO$_4$ was added to the bicarbonate solutions for pre-setting a κ_S of 23.0 ± 0.1 mS cm^{-1} and the experiments were conducted for 48 h. As the anolyte solution was refreshed permanently during all experiments, its κ_S value remained stable at *ca.* 5 mS cm^{-1}. Despite the occasional increases in r_{HCOO-} and CE (Fig. 5A), both performance parameters remained stable during the experiment. Although an increase in the κ_S was expected to influence the performance of the eCO$_2$RR, a MANOVA test showed that there was no correlation between the κ_S of the catholyte and r_{HCOO-} (p-value: 0.8909) or CE (p-value: 0.3177). Yet, again the change in κ_S affected the E_{WE} (p-value: 8.617 × 10^{-4}) and pH (p-value: 2.2 × 10^{-16}), which may in turn influence the performance (Fig. 5B).

3.5. It is not only catholyte, but also cathode surface

We showed that the longer-term operation of eCO$_2$RR is feasible, yet the best performance was only achieved over the first few hours. As shown above, this performance decrease seems mainly to be related to changes in c_{HCOO-} and κ_S of the catholyte. Therefore, we assumed that
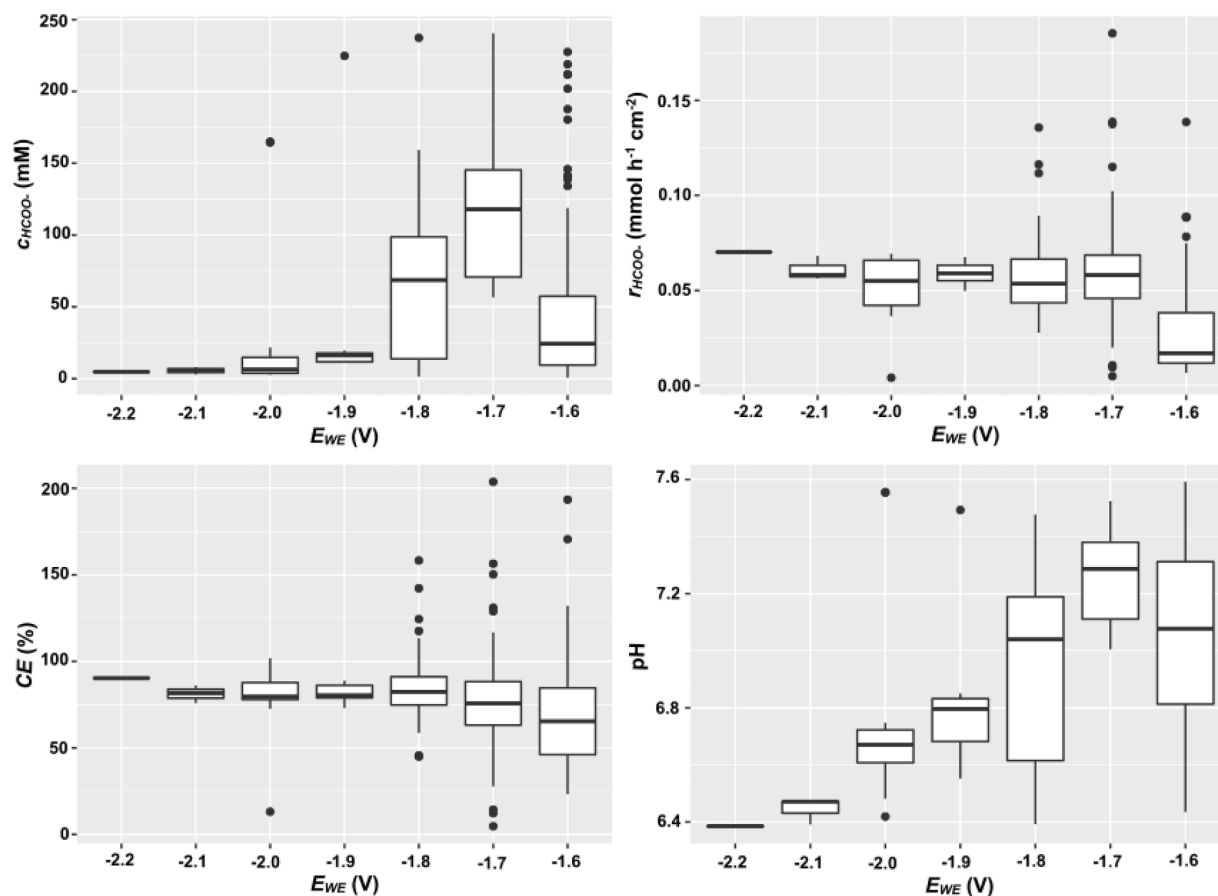
Fig. 3. Box-plots of formate concentration (c_{HCOO^-}) accumulated in the catholyte, formate production rate (r_{HCOO^-}), coulombic efficiency (*CE*) and pH at different actual cathode potentials (E_{WE}) denoted at the *x*-axis. All data are from 72 h electrochemical CO_2 reduction to formate at 4 different applied potentials ($E_{applied}$) of -2.2 V, -2.0 V, -1.8 V, and -1.6 V each performed in triplicate (n=3). In each box, horizontal black lines denote median values, extending from the 25th to the 75th percentile of each group's distribution of values. The error bars denote the 5th and 95th percentile values. Black dots denote the observations outside the range of adjacent values.

refreshing the catholyte should enhance or at least stabilize the performance. Thus, the catholyte was completely replaced with a fresh solution after 72 h of experiment in the reactors operated at the $E_{applied}$ of -2.2 V, and the operation was further carried out for another 28 h and the data monitored after 24 h was compared with the data collected from the first 24 h (first 24 h of 72 h-operation). In contrast to our expectations, lower *CE* (around 50%) and r_{HCOO^-} of 0.06 ± 0.02 mmol h^{-1} cm^{-2} were achieved during the further 24 h while the κ_S remaining below 21 mS cm^{-1} (Fig. S1). Thus, we hypothesized that the performance decline was as a result of corrosion of the electrocatalyst at the cathode surface during the first 72 h of operation. Catalyst corrosion and the resulting leaching of In to the catholyte is inevitable. Particularly at the cathode potentials needed for eCO$_2$RR having a high probability of HER leading to gas bubble formation and spalling off of metal particles. At carbon-based electrodes, the HER commonly starts at cathode potentials of -0.8 to -0.9 V [33]. At the surface of the electrode, particularly at the areas that In was probably not homogenously deposited, generated H$_2$ bubbles could cause In leaching in the catholyte. This was observed in the experiments. The corrosion rate was almost similar for $E_{applied}$ of -1.8, -2.0 and -2.2 V and increased after 72 h of operation to the average of 760 ng mL^{-1} day^{-1} or 15,248 ng cm^{-2} day^{-1} (Table S3). The slight differences in the corrosion values at different potentials (Table S3) were more likely related to the higher HER rate at more negative potentials. Predictably, the corrosion rates were much lower for $E_{applied}$ = -1.6 V (in average 18 ng mL^{-1} day^{-1} after 24 h to 44 ng mL^{-1} day^{-1} after 72 h). The competition of HER and eCO$_2$RR has been reported in previous studies using indium/indium oxide [34] as well as other types of

catalysts [35]. HER needs to be suppressed in order to achieve an efficient eCO$_2$RR. For instance, it was reported that increasing the mass transport in the system using the high-speed rotating gold electrode leads to an increase of eCO$_2$RR rather than HER by adjusting the pH at electrode surface [36]. In addition, some studies report that higher cathodic potentials (more negative) at indium can surprisingly be used to decrease the HER; even at a higher production rates of eCO$_2$RR [9].

3.6. Thermodynamic considerations

Accumulated formate and pH change could cause shifts in formal potentials of eCO$_2$RR, which can be calculated by the Nernst equation. An experimental measurement of formal potentials by approximating the midpoint of anodic and cathodic peaks using cyclic voltammetry can only be performed for reversible electrochemical reactions with low rate kinetics, which is not the case for the eCO$_2$RR [37]. Hence, formal potentials were calculated starting from the standard potential and using experimental conditions and saturated concentration of CO$_2$ [38]. Shift in the formal potential of eCO$_2$RR at different applied potentials and operational parameters found to be between -49 mV to -64 mV within the first 24 h of operation and around -78 mV to -93 mV for 72 h operation except the formate addition experiments resulting in lower shift of formal potential ($\approx$-30 mV at t=24 h, $\approx$-45 mV at t=48 h). Concentrations of both H$^+$ and HCOO$^-$ contributed to the shift in formal potential significantly, for instance formal potential shift of -84 ± 1 mV at the $E_{applied}$ of -2.2 V was recalculated under an assumed constant (initial) pH but at increased formate concentration as only -54 ± 6 mV.
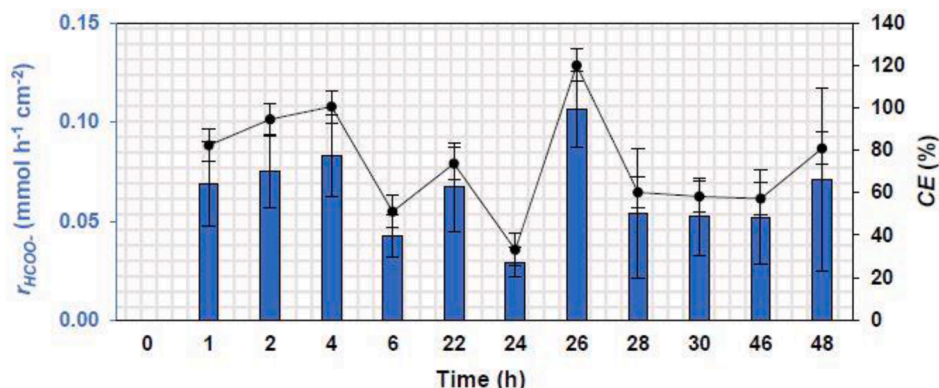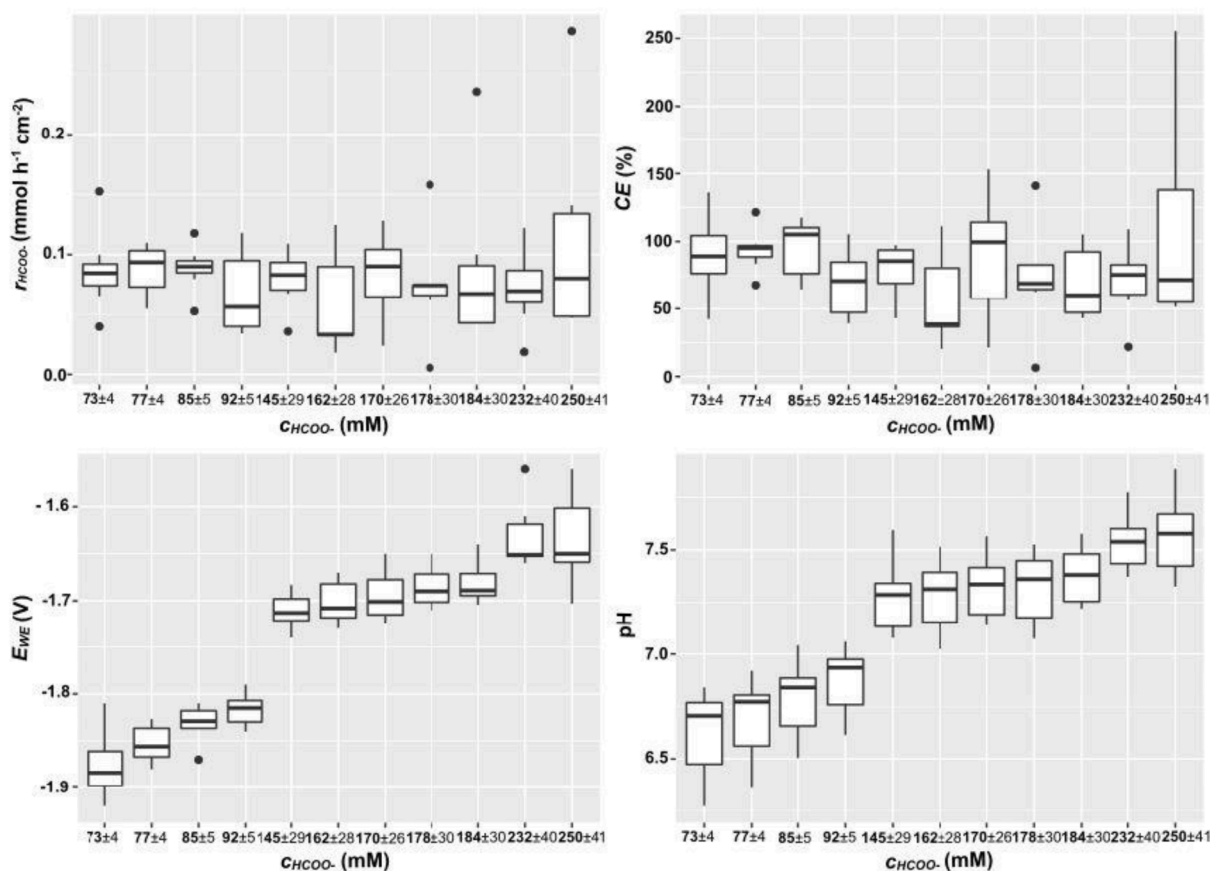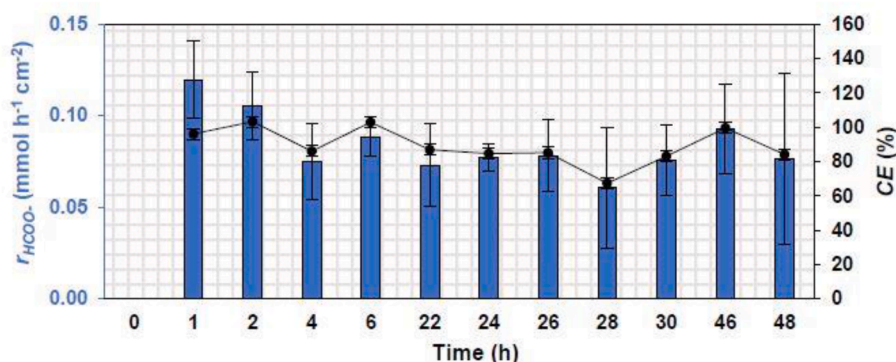
Fig. 4. A) Formate production rate (r_{HCOO-}) and coulombic efficiency (*CE*) during electrochemical CO_2 reduction to formate at the applied potential ($E_{applied}$) of -2.2 V with formate provided at *t*=0. All experiments were conducted for 48 h, in 0.05 M $NaHCO_3$ (pH 6.5) with formate concentration (c_{HCOO-}) of 70 mM as catholyte and 0.05 M $NaHCO_3$ (pH 6.5) as anolyte in quadruplicate (n=4). Reported values are mean values and the error bars represent the confidence interval ($\alpha = 0.05$). B) Box-plots of formate production rate (r_{HCOO-}), coulombic efficiency (*CE*), actual cathode potentials (E_{WE}) and pH at different c_{HCOO-} accumulated in the catholyte denoted at the *x*-axis. All the data are from 48 h electrochemical CO_2 reduction to formate at the $E_{applied}$ of -2.2 V with 70 mM formate provided in catholyte at *t*=0, performed in quadruplicate (n=4). In each box, horizontal black lines denote median values, extending from the 25th to the 75th percentile of each group's distribution of values. The error bars denote the 5th and 95th percentile values. Black dots denote the observations outside the range of adjacent values.

In summary, formal potential shifts were less than -100 mV for all eCO$_2$RR experiments (Table S11). Similar shifts in formal potential were observed for all potentials applied and experimental conditions, therefore the changes in *CE* are less likely to be explained thermodynamically. Formal potentials of eCO$_2$RR and HER also shift similarly during continuous reactor operation further indicating that any shift in

selectivity between eCO$_2$RR and HER is based on mechanistic or kinetic reasons, similar to the findings of the previous study with the same reactor setup [9].
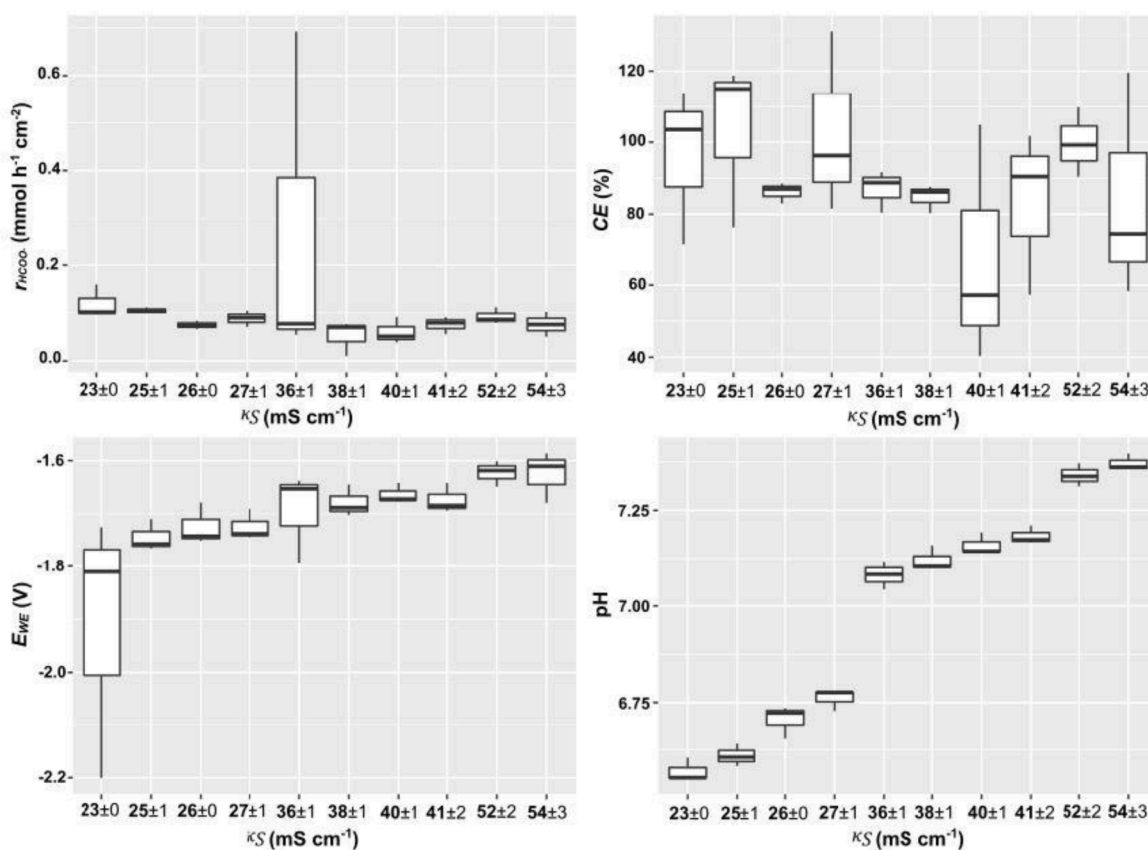
A)

B)

Fig. 5. A) Formate production rate (r_{HCOO^-}) and coulombic efficiency (*CE*) achieved during electrochemical CO_2 reduction to formate at the applied potential ($E_{applied}$) of -2.2 V with catholyte conductivity (κ_S) adjusted at *ca.* 23 mS cm^{-1} at *t*=0. All experiments were conducted for 48 h, in 0.05 M NaHCO$_3$ (pH 6.5) with 17 g L^{-1} Na$_2$SO$_4$ as catholyte and 0.05 M NaHCO$_3$ (pH 6.5) as anolyte in triplicate (n=3). Reported values are mean values and the error bars represent the confidence interval ($\alpha = 0.05$). B) Box-plots of formate production rate (r_{HCOO^-}), coulombic efficiency (*CE*), actual cathodic potentials (E_{WE}) and pH at different catholyte κ_S denoted at the *x*-axis. All the data are from 48 h electrochemical CO_2 reduction to formate at the $E_{applied}$ of -2.2 V with 17 g L^{-1} Na$_2$SO$_4$ provided in catholyte at *t*=0, performed in triplicate (n=3). In each box, horizontal black lines denote median values, extending from the 25th to the 75th percentile of each group's distribution of values. The error bars denote the 5th and 95th percentile values. Black dots denote the observations outside the range of adjacent values.

3.7. Implications of reactor design and operation

It was observed that changes in the catholyte especially in κ_S affected the E_{WE} leading to a difference in the set $E_{applied}$. This κ_S change is as a result of charge balancing ion transfer through the membrane between the compartments [39]. The CEM placed between the anodic and cathodic compartments is assumed to be cation selective, therefore the

cations (esp. Na$^+$) inevitably passes through the membrane from the anolyte to the catholyte. Yet, under biocompatible conditions not only cations but also anions are transferred through CEM from catholyte to the anolyte [40]. Besides, in addition to formate production, there could be some shifts between carbonate/bicarbonate equilibrium and concentrations. Consequently, the concentration of anions and cations in the catholyte increases during eCO$_2$RR. This was confirmed by not only

increase in κ_S, but also decrease in the internal resistance as EIS analysis showed (6 to 1 Ω, after 72 h experiment at $E_{applied}$ = -2.2 V). Therefore, the change in catholyte solution led to further changes in E_{WE}, and eventually the occasional fluctuations observed for the production rate and efficiency (also confirmed statistically). Interestingly, the cation transfer through the membrane during eCO$_2$RR was recently discussed to cause changes in the electrical double layer at the cathode, limiting the active sites required for eCO$_2$RR [41]. Therefore, the specific cations in the electrolytes have to be further taken into consideration. Anion exchange membranes (AEMs) are commonly not a suitable alternative to CEMs for eCO$_2$RR, due to the more likely crossover of formate [42]. The cation transfer through the CEM could be prevented by using a bipolar membrane (BPM) [43]. However, the larger cell potential required when using BPM (due to the lack of proton transfer through the membrane and the extra driven force required for water splitting reaction of 800 mV) is a significant disadvantage [31]. Alternatively, membraneless single chamber reactors could be used, but that would lead to new challenges such as preventing oxidation of formate at the CE. Additionally, increase in c_{HCOO^-} accumulated in the solution and its effect on the cathode E_{WE} could not be neglected. This could be potentially tackled by constant refreshing the catholyte during operation. However, in case of further downstream processes to separate formate from the catholyte, the concentrated formate in the electrolyte solution is more favourable for the separation of formate from the matrix solution [18].

In this study, we showed that eCO$_2$RR to formate in a two-chamber electrochemical cell using an In electrode can be operated over more than only few hours. Nevertheless, changes within the catholyte (e.g. κ_S and c_{HCOO^-}) and cathode (e.g. catalyst leaching) over the long run influence the eCO$_2$RR and eventually limit the performance. As some of these changes seem inevitable, keeping the performance constant during the long-term operation is a challenge with $E_{applied}$ being the key parameter. A very negative $E_{applied}$ has advantage of higher production rates, albeit a higher energy demand per product. More importantly it also leads to higher rate of catalyst leaching that is deteriorating the performance. If less negative $E_{applied}$ is set, it rather keeps the catalyst structure firmer during the operation, but only at lower production rate. Adjusting stability and performance needs a delicate balance, maybe also including pulse operation or (periodically) different $E_{applied}$. In addition to affecting the cathode, the changes in catholyte bring further challenges, for instance on charge balancing ion transfer through the membrane and changes in κ_S and formate accumulating over time. These challenges originate from the influence of κ_S and c_{HCOO^-} on the E_{WE}, and as shown here the set electrode potential does not remain stable and is in turn affecting the production rate and efficiency. Hence, the electrode potential during the long-term operation of eCO$_2$RR needs to be monitored and re-adjusted regularly.

3.8. Towards catalyst stability for long-term eCO$_2$RR operations

This study strongly highlights the importance of catalyst stability over long-term operation of eCO$_2$RR on the example of In cathodes. Stability of the electrocatalysts depends on the electrode architecture, but especially material. The exception are very few electrocatalysts for eCO$_2$RR such as Ag that showed high stability for conversion of CO$_2$ to syngas (>1200 h) [44]. In particular, the long-term stability of the electrodes with only In as the catalyst was not studied before. However, pulsed electrolysis has been shown as an effective method for Cu electrodes [45]. Cu containing electrocatalysts also suffer from only short-term stability and decreasing selectivity of eCO$_2$RR, e.g. for methane and ethylene [46]. This was mainly assigned to morphological changes in the electrocatalyst surface [5,47]. One possible causation for deactivation of the catalyst could be poisoning by deposition of the impurities from the solution on the catalyst surface. Although this was the case in some studies [47], no deposited impurities were found in other studies [48]. Adding pulsed oxidation as intermittent steps during

the eCO$_2$RR was reported to re-activate the catalyst. It was shown that the pulsed oxidation steps lead to formation of a "fresh" copper oxide layer at the surface of the electrode, allowing the formation of surface-bound intermediates favouring hydrocarbon production by eCO$_2$RR over HER [49]. The repeated cyclic voltammetry scans with anodic reverse potentials seemed to show similar results to pulsed oxidation steps, increasing the methane production by eCO$_2$RR to up to 50 h [48].

Another approach towards stability of electrodes and therefore long-term eCO$_2$RR operation is using bimetallic catalysts such as Cu-In, by decreasing the eCO$_2$RR overpotentials [7]. Depending on lattice compatibility of the metals, the bimetallic catalysts can be in form of alloy or heterostructure. An electronic interaction of the alloy catalysts and a synergistic interaction at the interfacial regions for the hetero-structured catalysts could enhance the adsorption of ●COOH species and weaken the adsorption of ●H species, leading to HER inhabitation [7]. Although the activity of the interfacial sites between the Cu and In in the Cu-In catalysts is not completely understood, the suppression of HER could be the reason for stability of Cu-In reported previously. For instance, the 7 h operation of Cu-In catalyst at -0.6 V vs. RHE in 0.1 M KHCO$_3$ with a selectivity of 95% towards CO was reported [50]. Operating eCO$_2$RR for 60 h with stable *CE* at 90% for CO production at the potentials of -0.6 to -0.8 V vs. RHE was achieved by Luo at al using Cu nanowires covered by a thin layer of In [51]. Long-term stability of In$_2$O$_3$/Cu$_2$O and In$_2$O$_3$/Cu$_3$N at -0.6 V vs. RHE in 0.1 M KHCO$_3$ was also reported. Being CO as the main product again, stable *CE* of 80% was achieved during 50 h eCO$_2$RR [52]. Many other cathodic electro-catalysts were tested in combination with In. One example is palladium (Pd)-In/three-dimensional graphene which showed the highest *CE* of 85% being stable for 24 h at -1.6 V vs. Ag/AgCl in 0.5 KHCO$_3$ [53]. The authors discussed the small particle size and high particle dispersion to be the reason for stable catalytic performance.

3.9. Integration of eCO$_2$RR and microbial synthesis

One of the main reasons of targeting formate production from CO$_2$ at biocompatible conditions is the role of formate as both carbon and energy sources for microbial metabolisms and further biosynthesis of value-added compounds [18,54]. According to previous successful studies on CO$_2$RR combining the electrochemical and microbial processes [19,55], the c_{HCOO^-}, r_{HCOO^-} and *CE* achieved in our study is sufficient for further biosynthesis using formate in case of integrating eCO$_2$RR and microbial synthesis. In fact, one of the factors causing changes in E_{WE} at the cathodic potentials of -1.8, -2.0 and -2.2 V was accumulation of formate in the catholyte, which could be tackled by simultaneous consumption of formate by microbial cells after its production through eCO$_2$RR. Nevertheless, two potential issues need to be considered and examined when integrating eCO$_2$RR and microbial synthesis. First, the catholyte used in our setup was only 0.05 M NaHCO$_3$, which does not provide an optimal condition for microbial growth and activities. If microbial media is used as a catholyte the high κ_S of the catholyte due to the additional chemicals vital for microbial growth will lead to more changes in E_{WE} and therefore the fluctuations in r_{HCOO^-} and *CE*, as observed in this study. Second, the single or bimetallic catalysts may provide toxicity for microbial cells particularly over the long run. Therefore, to what extend these two issues are affecting the eCO$_2$RR and further biosynthesis is a crucial question which needs to be systematically studied, in order to find optimal conditions favourable for both electrochemical and microbial processes. The answer to this question will potentially incite electrochemical and microbial technologies further towards industrial applications.

4. Conclusions

This study investigated the potential parameters limiting the stable eCO$_2$RR to formate using In catalyst over 72 h operation. We showed

that in order to achieve a stable and efficient eCO$_2$RR, the interrelation between few operational parameters needs to be taken into consideration. In the case studied here being exemplarily for interfacing eCO$_2$RR and bioproduction, a c_{HCOO^-} increase in the catholyte and change in κ_S of the catholyte may not directly influence the r_{HCOO^-} and CE. Yet, they affect the E_{WE}, leading to fluctuations in r_{HCOO^-} (maximum $\pm$ 0.03 mmol h^{-1} cm^{-2} at stable operation at each condition) and CE (max. $\pm$ 40% at stable operation at each condition) after reaching the certain value of c_{HCOO^-} and κ_S in the catholyte (*ca.* 70 mM and 21 mS cm^{-1}, respectively). Therefore, the concentration should be kept below such a value which can be easily achieved by process steering allowing balancing the rates of eCO$_2$RR and microbial consumption. In addition, the stability of the In catalyst needs to be improved in order to operate long-term stable eCO$_2$RR. Confirmed by the increase observed in In corrosion rate at more negative potentials and change in the pH values, H$_2$ generation at the surface could lead to the damage at the surface of the electrode coated by the electrocatalyst. Therefore, the durability of the electrode can be closely related to the electrode potential. One can consider less negative potentials to decrease the catalyst leaching but to increase the HER. However, that would consequently decrease r_{HCOO^-} from eCO$_2$RR. Alternatively, more C$_1$-compound selective electrodes can be explored and used.

CRediT authorship contribution statement

Paniz Izadi: Conceptualization, Methodology, Formal analysis, Investigation, Visualization, Writing – original draft. **Aykut Kas:** Formal analysis, Investigation, Writing – review & editing. **Philip Haus:** Investigation, Formal analysis. **Falk Harnisch:** Conceptualization, Methodology, Formal analysis, Supervision, Funding acquisition, Writing – review & editing.

Declaration of Competing Interest

The authors declare that they have no known competing financial interests or personal relationships that could have appeared to influence the work reported in this paper.

Data availability

Data will be made available on request.

Acknowledgement

Supplementary materials

Supplementary material associated with this article can be found, in the online version, at doi:10.1016/j.electacta.2023.142733.

References

[1] O.S. Bushuyev, P. De Luna, C.T. Dinh, L. Tao, G. Saur, J. van de Lagemaat, S. O. Kelley, E.H. Sargent, What should we make with CO2 and how can we make it? Joule 2 (2018) 825–832.

[2] D. Li, H. Zhang, H. Xiang, S. Rasul, J.-M. Fontmorin, P. Izadi, A. Roldan, S.F. R. Taylor, Y. Feng, L. Banerji, A.J. Cowan, E.H. Yu, J. Xuan, How to go beyond C1 products with electrochemical reduction of CO2, Sustainable Energy & Fuels (2021).

[3] A. Ruiz-Valencia, D. Benmeziane, N. Pen, E. Petit, V. Bonniol, M. Belleville, D. Paolucci, J. Sanchez-Marcano, L. Soussan, CO2 valorization by a new microbiological process, Catalysis Today 346 (2020) 106–111.

[4] J. Qiao, Y. Liu, F. Hong, J. Zhang, A review of catalysts for the electroreduction of carbon dioxide to produce low-carbon fuels, Chemical Society Reviews 43 (2014) 631–675.

[5] K.P. Kuhl, E.R. Cave, D.N. Abram, T.F. Jaramillo, New insights into the electrochemical reduction of carbon dioxide on metallic copper surfaces, Energy & Environmental Science 5 (2012) 7050–7059.

[6] L. Wu, K.E. Kolmeijer, Y. Zhang, H. An, S. Arnouts, S. Bals, T. Altantzis, J. P. Hofmann, M.C. Figueiredo, E.J. Hensen, Stabilization effects in binary colloidal Cu and Ag nanoparticle electrodes under electrochemical CO 2 reduction conditions, Nanoscale 13 (2021) 4835–4844.

[7] J. Li, M. Zhu, Y.F. Han, Recent advances in electrochemical CO2 reduction on indium-based catalysts, ChemCatChem 13 (2021) 514–531.

[8] K. Mou, Z. Chen, S. Yao, L. Liu, Enhanced electrochemical reduction of carbon dioxide to formate with in-situ grown indium-based catalysts in an aqueous electrolyte, Electrochimica Acta 289 (2018) 65–71.

[9] R. Hegner, L.F. Rosa, F. Harnisch, Electrochemical CO2 reduction to formate at indium electrodes with high efficiency and selectivity in pH neutral electrolytes, Applied Catalysis B: Environmental 238 (2018) 546–556.

[10] R. Hegner, K. Neubert, L.F. Rosa, F. Harnisch, Engineering electrochemical CO2 reduction to formate under bioprocess-compatible conditions to bioreactor scale, ChemElectroChem 6 (2019) 3731–3735.

[11] X. Sun, H.K. Atiyeh, R.L. Huhnke, R.S. Tanner, Syngas fermentation process development for production of biofuels and chemicals: A review, Bioresource Technology Reports 7 (2019), 100279.

[12] L.T. Angenent, H. Richter, W. Buckel, C.M. Spirito, K.J. Steinbusch, C.M. Plugge, D. P. Strik, T.I. Grootscholten, C.J. Buisman, H.V. Hamelers, Chain elongation with reactor microbiomes: open-culture biotechnology to produce biochemicals, Environmental science & technology 50 (2016) 2796–2810.

[13] W. de Araújo Cavalcante, R.C. Leitão, T.A. Gehring, L.T. Angenent, S.T. Santaella, Anaerobic fermentation for n-caproic acid production: A review, Process Biochemistry 54 (2017) 106–119.

[14] M. Roghair, T. Hoogstad, D.P. Strik, C.M. Plugge, P.H. Timmers, R.A. Weusthuis, M.E. Bruins, C.J. Buisman, Controlling ethanol use in chain elongation by CO2 loading rate, Environmental science & technology 52 (2018) 1496–1505.

[15] N. Wan, A. Sathish, L. You, Y.J. Tang, Z. Wen, Deciphering Clostridium metabolism and its responses to bioreactor mass transfer during syngas fermentation, Scientific reports 7 (2017) 1–11.

[16] Q. Fei, M.T. Guarnieri, L. Tao, L.M. Laurens, N. Dowe, P.T. Pienkos, Bioconversion of natural gas to liquid fuel: opportunities and challenges, Biotechnology Advances 32 (2014) 596–614.

[17] P. Izadi, E. Yu, Realizing Full Potential of Bioelectrochemical and Photoelectrochemical Systems, Joule 4 (2020) 2085–2087.

[18] P. Izadi, F. Harnisch, Microbial| electrochemical CO2 reduction: To integrate or not to integrate? Joule 6 (2022) 935–940.

[19] H. Li, P.H. Opgenorth, D.G. Wernick, S. Rogers, T.-Y. Wu, W. Higashide, P. Malati, Y.-X. Huo, K.M. Cho, J.C. Liao, Integrated electromicrobial conversion of CO2 to higher alcohols, Science 335 (2012) 1596, 1596.

[20] M. Stöckl, S. Harms, I. Dinges, S. Dimitrova, D. Holtmann, From CO2 to Bioplastic–Coupling the Electrochemical CO2 Reduction with a Microbial Product Generation by Drop-in Electrolysis, ChemSusChem 13 (2020) 4086–4093.

[21] K.R. Chatzipanagiotou, L. Jourdin, C.J. Buisman, D.P. Strik, J.H. Bitter, CO2 Conversion by Combining a Copper Electrocatalyst and Wild-type Microorganisms, ChemCatChem 12 (2020) 3900–3912.

[22] C. Gimkiewicz, R. Hegner, M.F. Gutensohn, C. Koch, F. Harnisch, Study of electrochemical reduction of CO2 for future use in secondary microbial electrochemical technologies, ChemSusChem 10 (2017) 958–967.

[23] W. Luo, W. Xie, M. Li, J. Zhang, A. Züttel, 3D hierarchical porous indium catalyst for highly efficient electroreduction of CO 2, Journal of Materials Chemistry A 7 (2019) 4505–4515.

[24] F. Bienen, A. Löwe, J. Hildebrand, S. Hertle, D. Schonvogel, D. Kopljar, N. Wagner, E. Klemm, K.A. Friedrich, Degradation study on tin-and bismuth-based gas-diffusion electrodes during electrochemical CO2 reduction in highly alkaline media, Journal of Energy Chemistry 62 (2021) 367–376.

[25] W. Ma, S. Xie, X.-G. Zhang, F. Sun, J. Kang, Z. Jiang, Q. Zhang, D.-Y. Wu, Y. Wang, Promoting electrocatalytic CO2 reduction to formate via sulfur-boosting water activation on indium surfaces, Nature communications 10 (2019) 1–10.

[26] J. Barek, A.G. Fogg, A. Muck, J. Zima, Polarography and voltammetry at mercury electrodes, Critical reviews in analytical chemistry 31 (2001) 291–309.

[27] W.M. Haynes, D.R. Lide, T.J. Bruno, CRC handbook of chemistry and physics, CRC press (2016).

[28] R.C. Team, R Core Team R. R, A Language and Environment for Statistical Computing R Foundation for Statistical Computing, Vienna, Austria, 2016.

[29] R.C. Team, R: A language and environment for statistical computing [Computer software manual], Vienna, Austria, 2019.

[30] H. Wickham, W. Chang, M.H. Wickham, Package 'ggplot2', Create elegant data visualisations using the grammar of graphics, Version 2 (2016) 1–189.

[31] R.A. Tufa, D. Chanda, M. Ma, D. Aili, T.B. Demissie, J. Vaes, Q. Li, S. Liu, D. Pant, Towards highly efficient electrochemical CO2 reduction: Cell designs, membranes and electrocatalysts, Applied Energy 277 (2020), 115557.

[32] R.A. Rozendal, H.V. Hamelers, R.J. Molenkamp, C.J. Buisman, Performance of single chamber biocatalyzed electrolysis with different types of ion exchange membranes, Water research 41 (2007) 1984–1994.

[33] P. Izadi, J.-M. Fontmorin, A. Godain, H.Y. Eileen, I.M. Head, Parameters influencing the development of highly conductive and efficient biofilm during microbial electrosynthesis: the importance of applied potential and inorganic carbon source, npj Biofilms and Microbiomes 6 (2020) 1–15.

[34] W. Yang, Y. Zhao, S. Chen, W. Ren, X. Chen, C. Jia, Z. Su, Y. Wang, C. Zhao, Defective Indium/Indium Oxide Heterostructures for Highly Selective Carbon Dioxide Electrocatalysis, Inorganic Chemistry 59 (2020) 12437–12444.

[35] M.C.O. Monteiro, A. Goyal, P. Moerland, M.T.M. Koper, Understanding Cation Trends for Hydrogen Evolution on Platinum and Gold Electrodes in Alkaline Media, ACS Catalysis 11 (2021) 14328–14335.

[36] A. Goyal, G. Marcandalli, V.A. Mints, M.T.M. Koper, Competition between CO2 Reduction and Hydrogen Evolution on a Gold Electrode under Well-Defined Mass Transport Conditions, Journal of the American Chemical Society 142 (2020) 4154–4161.

[37] J. Ho, M.L. Coote, C.J. Cramer, D.G. Truhlar, 6 Theoretical Calculation of Reduction Potentials, (2015).

[38] J.G. Speight, Lange's handbook of chemistry, McGraw-Hill Education, 2017.

[39] M. Ramdin, A.R. Morrison, M. De Groen, R. Van Haperen, R. De Kler, L.J. Van Den Broeke, J.M. Trusler, W. De Jong, T.J. Vlugt, High pressure electrochemical reduction of CO2 to formic acid/formate: a comparison between bipolar membranes and cation exchange membranes, Industrial & engineering chemistry research 58 (2019) 1834–1847.

[40] F. Harnisch, U. Schröder, Selectivity versus mobility: separation of anode and cathode in microbial bioelectrochemical systems, ChemSusChem: Chemistry & Sustainability Energy & Materials 2 (2009) 921–926.

[41] B. Pan, Y. Wang, Y. Li, Understanding and leveraging the effect of cations in the electrical double layer for electrochemical CO2 reduction, Chem Catalysis (2022).

[42] H. Strathmann, A. Grabowski, G. Eigenberger, Ion-exchange membranes in the chemical process industry, Industrial & Engineering Chemistry Research 52 (2013) 10364–10379.

[43] D.A. Salvatore, D.M. Weekes, J. He, K.E. Dettelbach, Y.C. Li, T.E. Mallouk, C.P. Berlinguette, Electrolysis of Gaseous CO2 to CO in a Flow Cell with a Bipolar Membrane, ACS Energy Letters 3 (2017) 149–154.

[44] T. Haas, R. Krause, R. Weber, M. Demler, G. Schmid, Technical photosynthesis involving CO2 electrolysis and fermentation, Nature Catalysis 1 (2018) 32–39.

[45] Y. Jännsch, J.J. Leung, M. Hämmerle, E. Magori, K. Wiesner-Fleischer, E. Simon, M. Fleischer, R. Moos, Pulsed potential electrochemical CO2 reduction for enhanced stability and catalyst reactivation of copper electrodes, Electrochemistry Communications 121 (2020), 106861.

[46] K. Schouten, Y. Kwon, C. Van Der Ham, Z. Qin, M. Koper, A new mechanism for the selectivity to C 1 and C 2 species in the electrochemical reduction of carbon dioxide on copper electrodes, Chemical Science 2 (2011) 1902–1909.

[47] Y. Hori, H. Konishi, T. Futamura, A. Murata, O. Koga, H. Sakurai, K. Oguma, Deactivation of copper electrode" in electrochemical reduction of CO2, Electrochimica acta 50 (2005) 5354–5369.

[48] B. Jermann, J. Augustynski, Long-term activation of the copper cathode in the course of CO2 reduction, Electrochimica acta 39 (1994) 1891–1896.

[49] A. Engelbrecht, C. Uhlig, O. Stark, M. Hämmerle, G. Schmid, E. Magori, K. Wiesner-Fleischer, M. Fleischer, R. Moos, On the electrochemical CO2 reduction at copper sheet electrodes with enhanced long-term stability by pulsed electrolysis, Journal of The Electrochemical Society 165 (2018) J3059.

[50] S. Rasul, D.H. Anjum, A. Jedidi, Y. Minenkov, L. Cavallo, K. Takanabe, A highly selective copper–indium bimetallic electrocatalyst for the electrochemical reduction of aqueous CO2 to CO, Angewandte Chemie 127 (2015) 2174–2178.

[51] W. Luo, W. Xie, R. Mutschler, E. Oveisi, G.L. De Gregorio, R. Buonsanti, A. Züttel, Selective and stable electroreduction of CO2 to CO at the copper/indium interface, Acs Catalysis 8 (2018) 6571–6581.

[52] G.O. Larrazábal, T. Shinagawa, A.J. Martín, J. Pérez-Ramírez, Microfabricated electrodes unravel the role of interfaces in multicomponent copper-based CO2 reduction catalysts, Nature Communications 9 (2018) 1477.

[53] G. He, H. Tang, H. Wang, Z. Bian, Highly selective and active Pd-In/three-dimensional graphene with special structure for electroreduction CO2 to formate, Electroanalysis 30 (2018) 84–93.

[54] M. Stöckl, N. Claassens, S. Lindner, E. Klemm, D. Holtmann, Coupling electrochemical CO2 reduction to microbial product generation–identification of the gaps and opportunities, Current Opinion in Biotechnology 74 (2022) 154–163.

[55] Y. Tashiro, S. Hirano, M.M. Matson, S. Atsumi, A. Kondo, Electrical-biological hybrid system for CO2 reduction, Metabolic engineering 47 (2018) 211–218.